

Routing with Self-Attention for Multimodal Capsule Networks

Kevin Duarte¹ Brian Chen² Nina Shvetsova³ Andrew Rouditchenko⁴ Samuel Thomas^{5,6}
Alexander Liu⁴ David Harwath⁷ James Glass⁴ Hilde Kuehne^{3,6} Mubarak Shah¹

¹University of Central Florida, ²Columbia University, ³Goethe University Frankfurt, ⁴MIT CSAIL,

⁵IBM Research AI, ⁶MIT-IBM Watson AI Lab, ⁷UT Austin

kevin.duarte@knights.ucf.edu, bc2754@columbia.edu, {shvetsov, kuehne}@uni-frankfurt.de
{roudi, glass}@mit.edu, sthomas@us.ibm.com, harwath@cs.utexas.edu, shah@crcv.ucf.edu

Abstract

The task of multimodal learning has seen a growing interest recently as it allows for training neural architectures based on different modalities such as vision, text, and audio. One challenge in training such models is that they need to jointly learn semantic concepts and their relationships across different input representations. Capsule networks have been shown to perform well in context of capturing the relation between low-level input features and higher-level concepts. However, capsules have so far mainly been used only in small-scale fully supervised settings due to the resource demand of conventional routing algorithms. In this work, we propose a new multimodal capsule network that allows us to leverage the strength of capsules in the context of a multimodal learning framework on large amounts of video data. To adapt the capsules to large-scale input data, we propose a novel routing by self-attention mechanism that selects relevant capsules which are then used to generate a final joint multimodal feature representation. This allows not only for robust training with noisy video data, but also to scale up the size of the capsule network compared to traditional routing methods while still being computationally efficient. We evaluate the proposed architecture by pretraining it on a large-scale multimodal video dataset and applying it on four datasets in two challenging downstream tasks. Results show that the proposed multimodal capsule network is not only able to improve results compared to other routing techniques, but also achieves competitive performance on the task of multimodal learning.

1. Introduction

With the proliferation of video sharing websites and affordable recording devices, the amount of video data available today has dramatically increased. Given that hand annotating this continuously growing stream of data is infea-

sible, recent research has turned to training networks on such large-scale multimodal data without manual annotation [3, 35, 36]. These works make use of the fact that large amounts of data are available across multiple modalities such as vision, text, and audio, especially like in case of videos. Beyond learning better feature representations by pretraining on large datasets [3], such networks are able to relate cross-modal inputs based on the similarity of their internal neural representations [2, 35], which can be applied to zero-shot tasks like classification or text-to-video retrieval. Especially for the latter case, it becomes necessary to capture similar semantic relationships across very different and low level feature representations, as e.g. video features extracted by a ResNet architecture [21] have to be related to bag of words representations of sentences [35], or even sound representations extracted from audio waveforms [41]. These relationships can be captured by training a network that takes pairs of modalities as inputs and predicts a similarity score, or by projecting both representations into a joint embedding space. In the second case, for example, the encoding for a sentence like “Cut the chicken.” would be close to the visual representation’s encoding of frames showing this activity and further away from the encoding of frames showing other objects like vegetables or unrelated topics like outdoor activities. The semantic closeness can then be measured based on distance metrics (e.g. by simple dot product).

Learning such a joint embedding space involves the grouping of similar concepts across different modalities. Here, it can be helpful to identify which low-level features show activation in certain contexts, which can serve as a form of filtering to focus on relevant inputs and thus learn a good joint embedding space. Capsule networks [42] have been proposed as a technique to capture activations of a specific type of entity and to model higher-level objectness from groups of low-level feature activations. To this end, capsule networks find familiar concepts by perform-

ing “high-dimensional coincidence filtering” [23] through a routing-by-agreement algorithm. They have shown their ability in modeling these relationships in images [23,26,42] and videos [15], and have also performed well in multimodal applications [34, 45]. However, those approaches have thus far mainly been applied in a fully supervised setting with clean data.

In this work, we leverage the qualities of capsule architectures in the context of multimodal learning to learn a joint embedding space across different input modalities. To allow the capsules to learn from large-scale noisy input data, we propose an efficient routing by self-attention mechanism that finds similarity between these lower-level capsule representations to produce higher-level capsules and activations. To this end, we build upon the standard capsule network setup and generate a set of capsules for the input features. From these capsules, we obtain votes for higher-level capsules, in the form of key-query-value tuples, and perform a self attention operation to obtain the higher-level capsule pose representations. These are then passed through a linear layer and a softmax layer to obtain the final activations. These activations are used to select relevant capsules, increasing the impact of those feature groups belonging to certain object representations while reducing the impact for irrelevant ones. We find that this self-attention based routing mechanism is more scalable than standard dynamic [42] and EM [23] routing methods: this is vital for applying capsule networks to large-scale video datasets.

The proposed multimodal capsule network is trained by mapping the selected capsules to a joint multimodal embedding space which is enforced by the use of a contrastive loss. For evaluation, we train the system on the HowTo100M multimodal dataset, consisting of 1.2 million YouTube instruction videos and evaluate the resulting method on the two zero-shot down-stream tasks of video retrieval on the YouCook2 [50] and MSR-VTT [46] dataset and action localization on the CrossTask [52] and the MiningYouTube [27] dataset. Our experiments show that the proposed architecture is able to improve performance compared to existing routing mechanisms and to provide competitive performance on all evaluated downstream tasks.

The contributions of the paper are as follows:

- To the best of our knowledge, we are the first to leverage the benefits of capsule architectures for large-scale multimodal data without human annotation.
- To this end we propose a novel routing by self-attention mechanism for capsule architectures.
- We show that the proposed mechanism is more efficient and scalable than other routing techniques, achieving state-of-the-art results on various challenging benchmark tasks.

2. Related Work

Multimodal Learning As annotating large datasets [10, 13], especially video, is extremely costly, recent approaches started take advantage of the vast amount of video data on websites and social media platforms by leveraging readily available tools like automatic speech recognition systems. This allows the creation of narrated video datasets [36, 43]. Following that, various methods have been proposed to learn from two or more input modalities, e.g. video-text pairs [5, 14, 17, 30, 32, 40, 44, 51], video-audio pairs [4, 6, 8, 41], or all three modalities, video, audio, and text [2, 11]. Most methods use the large-scale data for pretraining the network followed by a fine-tuning on a downstream dataset, which is usually done with less noisy curated or hand-annotated data [4, 14, 30, 32, 40, 41]. However, some approaches show that training on large-scale noisy data alone can also be sufficient and directly apply the model without fine-tuning on the downstream datasets [5,8,17,40,44]. Especially in the later case, training is usually realized with some variant of a contrastive loss function, such as noise contrastive estimation (NCE) used by [36] or Masked Margin Softmax (MMS) used by [41]. Other methods such as XDC [4] and MCN [11] argue that embedding space learning can be improved by also adding a clustering component to the contrastive loss to form groups with similar representations in the embedding space but it usually comes at the cost of having an additional Sinkhorn [12] or K-means [31] clustering in the pipeline. Our proposed method picks up on this idea, but instead of having an explicit clustering objective at the end of the pipeline, we use the implicit characteristics of capsule networks (*i.e.* routing-by-agreement) to group concepts at an earlier stage of the network. Technically, most approaches rely on either convolutional architectures [2, 4–6, 8, 11, 36, 41], self-attention mechanisms [17, 30, 32, 44, 51] or a combination thereof [40]. To the best of our knowledge, this work makes a first attempt, to employ the abilities of capsule networks to address the problem of multimodal self-supervised learning. The proposed approach uses self-attention as an efficient routing mechanism to attend to relevant elements (*i.e.* capsules) in large-scale data.

Capsule Networks The concept of capsule networks was first introduced in [22], where view-equivariant vector representations were learned from images. Sabour *et al.* [42] extended this idea and proposed an iterative routing-by-agreement algorithm which was able to classify and segment overlapping digits. Capsule networks have been widely applied to various domains and problems including text classification [47], video action detection [15], point cloud processing [49], and medical image segmentation [28]. One key aspect of capsules networks is their abil-

ity to route and hierarchically activate higher-level capsules based on agreement of multiple lower-level capsules. However, this ability comes with the increased computational cost of the routing-by-agreement algorithm. First capsule architectures [42] used dynamic routing which can be computationally slow and results in high memory consumption, especially on higher dimensional input data and for a larger number of capsules. Hinton *et al.* [23] reduced the number of parameters by learning matrix capsules with an iterative Expectation-Maximization (EM) based routing algorithm. Several other works have attempted to make more efficient and scalable routing algorithms including self-routing capsule networks [18], KDE-based routing [48], STAR-Caps [1], spectral capsule networks [7], and subspace capsule networks [16]. Recently, Efficient-CapsNet [33] and stacked capsule autoencoders (SCAEs) [26] have proposed routing mechanisms based on attention. Efficient-CapsNet uses vector capsules similar to those found in [42], and computes self-attention across votes of the lower-level capsule layers to find the routing/coupling coefficients. Then, the resulting higher-level capsules are a weighted sum across these same votes based on the coefficients. Contrarily, our proposed self-attention routing method generates separate key, query, and value representations. This allows us to separate the computation of the votes and the routing coefficients: the key and query generate the routing coefficients, which are used to weight the votes to obtain the higher-level capsules. SCAEs adapt the Set Transformer [29] to perform routing between the set of part capsules to the object capsules. They generate capsule activations by maximizing the part pose likelihood from a mixture of predictions from lower-level capsules. Different from SCAE, we propose to use self-attention as a routing mechanism and we compute activation probabilities by the linear transformation of the higher level features followed by a softmax. We find this setting to be computationally more efficient allowing us to train without the need for tuning of sparsity constraints, while showing higher performance compared to Set Transformer in the targeted setup (see Sec. 4.4).

3. Multimodal Learning with Capsule Networks

In the following, we first describe the proposed multimodal capsule network architecture (Figure 1) at high level, and then follow with a detailed description of the proposed routing by self-attention mechanism (Figure 2). We close with a description of the training procedure.

System setup Given n video clips, each with a corresponding video, audio, and text representations we attempt to learn a joint multimodal representation space. We denote the video as $v \in \mathcal{V}$, the audio as $a \in \mathcal{A}$, and the text narration generated by an automated speech recognition (ASR)

system as $t \in \mathcal{T}$. Thus, the training set of n video clips is represented by tuples $\{(v_i, a_i, t_i)\}_{i=1}^n$. Contrastive multimodal learning attempts to learn a set of functions to generate embeddings for each modality such that embeddings for semantically similar inputs are closer together than semantically dissimilar inputs. Formally, we learn functions, $f_v : \mathcal{V} \rightarrow \mathbb{R}^D$, $f_a : \mathcal{A} \rightarrow \mathbb{R}^D$, and $f_t : \mathcal{T} \rightarrow \mathbb{R}^D$ which create D dimensional embeddings (i.e. $f_v(v) \in \mathbb{R}^D$). The input representations take the form of pre-extracted 2D and 3D features from a video clip, log-mel spectrograms extracted from an audio segment, and a text embedding extracted by sentence-based neural network. The goal is to find mapping functions f_v , f_a , and f_t , so that the distance of all possible pairs from the same tuple (v_i, a_i) , (t_i, a_i) , and (v_i, t_i) is minimized in the embedding space and the distance to all other tuple pairs is maximized. An overview of the overall system is shown in Figure 1.

3.1. Multimodal Capsule Architecture

Primary Capsules To learn the mapping of each input feature to the joint embedding space, i.e. functions f_v , f_a , and f_t , we propose a novel capsule network architecture. A capsule is composed of a multi-dimensional pose vector x , which represents an entity’s properties and an activation p , which represents an existence probability (i.e. the probability that the given entity/object exists within the input). From each input modality feature, a learned linear layer extracts a set of C primary capsule poses; the C activations are produced by a linear layer followed by a sigmoid non-linearity. We denote the i -th capsule for modality m has the pose vector $x_i^m \in \mathbb{R}^{d_1}$ and activation $p_i^m \in [0, 1]$. We use these capsules in a self-attention based routing-by-agreement algorithm, depicted in Figure 2, to learn the relationships between the entities they model.

Routing by Self-Attention Routing is the method by which capsule networks propagate information from one layer to the next. It is a type of voting mechanism which obtains votes from capsules in a lower capsule layer, and finds agreement between these votes which are aggregated into capsules in the higher capsules layer. To this end, traditional routing approaches (e.g. dynamic and EM routing) find agreement in high-dimensional space so that sets of lower level capsules can vote for higher-level capsules. This process is computationally expensive as it often relies on an iterative procedure, and has therefore mainly been used on small-scale data. We propose to replace this routing mechanism by utilizing self-attention, as self-attention can provide a similar mechanism for finding agreement between high-dimensional vectors.

Practically, we first multiply capsule pose vectors x_i^m by their respective activations p_i to ensure entities which are not present (i.e. $p_i^m \rightarrow 0$) are not used in the routing process. We then learn a set of functions to extract the re-

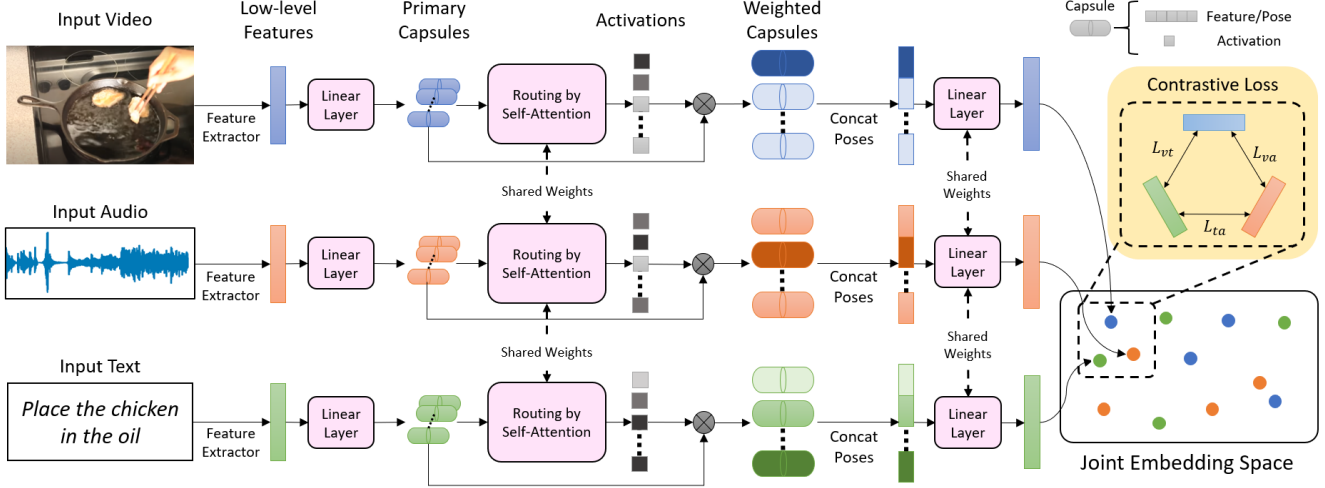


Figure 1. **Overview of our proposed approach.** Given a video, audio, and text triplet, the network extracts modality specific features and converts them into a set of primary capsules. Then, these capsules are routed using self-attention to obtain a higher-level activations, which are used to weight capsule features. The weighted capsule features are projected into a final joint multimodal feature representation. This joint representation space is enforced by a pair-wise contrastive loss.

spective key, query, and value representations from capsules $K = h_K(p_i^m x_i^m)$, $Q = h_Q(p_i^m x_i^m)$, $V = h_V(p_i^m x_i^m)$, using two linear layers for all functions h . These learned functions, $h_K, h_Q, h_V : \mathbb{R}^{d_1} \rightarrow \mathbb{R}^{d_2}$, map the primary capsule pose vectors to the secondary capsules’ pose feature space and are used in a multi-head self-attention mechanism:

$$\hat{x}_i^m = \text{Attention}(Q, K, V) = g\left(\text{softmax}\left(\frac{QK^T}{\sqrt{d_2}}\right)V\right), \quad (1)$$

where g is a two-layer nonlinear MLP¹. In the context of capsule routing, the query and key produce the routing coefficients which determine the amount of information a lower-level capsule sends a specific higher level capsule, whereas the value can be considered a vote, or prediction, for the properties of the higher level capsule.

From the secondary capsule layer’s poses, \hat{x}_i^m , we obtain their existence probabilities, through a softmax operation:

$$\hat{p}_i^m = \frac{\exp(x_i^m W_p + b_p)}{\sum_{j=1}^C \exp(x_j^m W_p + b_p)}, \quad (2)$$

where $W_p \in \mathbb{R}^{d_2 \times 1}$ and $b_p \in \mathbb{R}$ are learned parameters. These probabilities are used to select relevant capsules.

By analysing these existence probabilities for different inputs, we find that these higher-level capsules seem to capture and weight the existence of certain concepts at different granularity levels: some capsules represent general concepts “outdoors” or “video games”, while others are more specific like “paper folding” or “putting things in bowls”. A detailed discussion can be found in Section 4.5.

¹See Appendix for additional details

Mapping to Joint Embedding Space To finally map all capsules to a joint embedding space, we concatenate the activation-weighted capsules to a single vector and pass them through a linear transformation, f_{out} to obtain the final feature representations:

$$f_v = f_{\text{out}}(\hat{p}_i^v x_i^v), f_a = f_{\text{out}}(\hat{p}_i^a x_i^a), \text{ and } f_t = f_{\text{out}}(\hat{p}_i^t x_i^t). \quad (3)$$

Note that all learned weights used after the generation of the primary capsule layer, namely h_K, h_Q, h_V and f_{out} , are shared across modalities.

3.2. Contrastive Multimodal Learning

To train the described architecture and learn the joint representation space, we use a contrastive loss on each pair of modalities (v, a) , (t, a) , and (v, t) . For different modalities from the same video clip, the contrastive loss maximizes the similarity of their embeddings; conversely, it minimizes the similarity for embeddings from different video clips. Following [41], we use the Masked Margin Softmax (MMS) loss [24], which defines the dot-product between two vectors as the similarity measure and computes similarities across a batch of B samples.

The loss is computed between two modalities, and can be viewed as the sum of two instances of InfoNCE [39] (with a margin δ). For example, the loss for the visual/audio pair (L_{va}) consists of two components: the first where the visual input is fixed and audio samples are varied, and the second where the audio input is fixed and visual samples are varied.

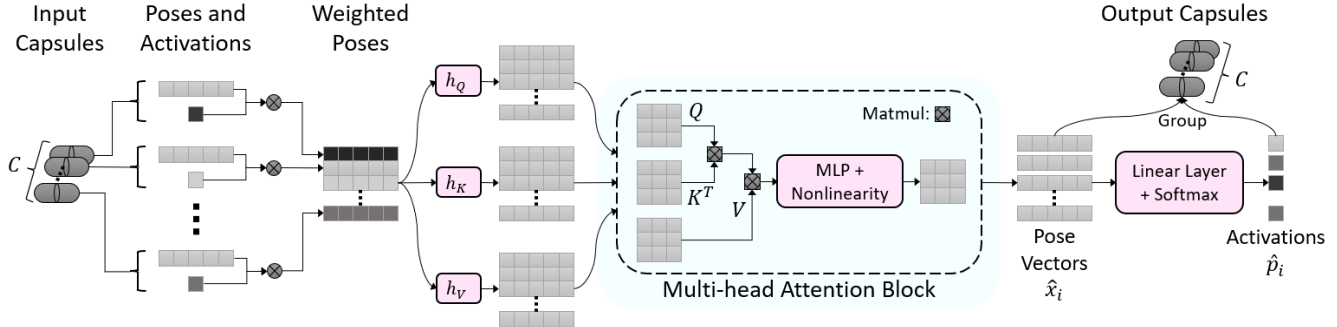


Figure 2. **Proposed Routing by Self-Attention.** The input is a set of C capsules. The activation-weighted capsule features are projected into query, key, and value matrices which are used in a multi-head self-attention block to generate higher-level capsule poses. A linear transformation with softmax activation then generates the activations for these higher-level capsules.

For the video-audio pair the loss is defined as:

$$L_{va} = \frac{1}{B} \sum_{i=1}^B \log \frac{e^{f_v(v_i) \cdot f_a(a_i) - \delta}}{e^{f_v(v_i) \cdot f_a(a_i) - \delta} + \sum_{\substack{j=1 \\ j \neq i}}^B e^{f_v(v_j^{\text{imp}}) \cdot f_a(a_i)}} + \log \frac{e^{f_v(v_i) \cdot f_a(a_i) - \delta}}{e^{f_v(v_i) \cdot f_a(a_i) - \delta} + \sum_{\substack{k=1 \\ k \neq i}}^B e^{f_v(v_i) \cdot f_a(a_k^{\text{imp}})}}, \quad (4)$$

where δ is an empirically selected hyper-parameter. Here, v_j^{imp} and a_k^{imp} are “imposters” (i.e. samples from the batch and do not co-occur within the same time-frame) from the video and audio modalities, respectively. For this video-audio case, the loss discriminates between the true embedding pairs (v_i, a_i) and the imposter pairs (v_k^{imp}, a_i) and (v_i, a_j^{imp}) , for all $k \neq i$ and $j \neq i$ in the batch. We sample negatives from both within the same video and from other videos, since this has been shown to empirically improve performance [36]. The final loss is the sum of the pairwise MMS losses between different modalities:

$$L_{\text{final}} = L_{va} + L_{ta} + L_{vt}. \quad (5)$$

Since the loss is computed over all modality pairs, it ensures all features are projected into the same space and are comparable.

4. Experimental Evaluation

In this section, we assess the performance of the proposed approach in the context of multimodal learning. For this evaluation, we focus on the zero shot capabilities of the proposed approach, namely on the downstream tasks of zero-shot text-to-video retrieval and zero-shot temporal action localization, as this allows us to evaluate how well high-level semantic concepts have been identified and

grouped across various modalities. We first present an overview on the implementation details of our proposed approach. The overall system performance is then compared with various other techniques in the field. We finally evaluate the impact of each component including the routing mechanism in comparison with other available techniques and present qualitative results for the proposed method. The code and related resources is publicly available at <https://github.com/KevinDuarte/Multimodal-Capsule-Networks>.

4.1. Implementation Details

Following [36], the input visual features for our method are 2D features extracted at 1 fps using a ResNet-152 model [21] pretrained on ImageNet [13], as well as 3D features extracted at 1.5 fps using a ResNext-101 [19] pretrained on Kinetics [10]. These features are max-pooled over time and concatenated to form a 4096 dimension feature vector for a given video clip. The audio input to our network are features extracted from the log-mel spectrograms by a pre-trained DAVENet model [20]. For textual features, we follow [36], and use a GoogleNews pretrained Word2vec model [37] to extract word embeddings. Then a max-pooling operation over all word embeddings in a sentence produces a single vector representation. All feature extraction backbones are fixed (i.e. not fine-tuned) during training and evaluation. To train our network we use an Adam optimizer [25] with a learning rate of 0.001 and cosine learning rate scheduler [38]. The model is trained on 4 V100 GPUs for 20 epochs, using a batch size of 4096. In the MMS loss, we set $\delta = 0.001$. Unless otherwise stated, we set the number of capsules to $C = 128$, the dimension of each capsule’s pose vector to $d_1 = 32$ and $d_2 = 256$, and the final joint representation dimension is $D = 4096$. Our method is trained using the HowTo100M [36] instructional video dataset, which consists of 1.2 million videos with corresponding audio and text transcripts extracted using an off-the-shelf ASR system. The video-audio-text tu-

Table 1. Evaluation of zero-shot text-to-video retrieval. MIL-NCE* uses the same training procedure as [35] with different backbone features, † indicates trainable backbone. Modality indicates the modalities used during inference, where V: video, T: text, A: audio.

Method	Modality	Visual Backbone	YouCook2				MSR-VTT			
			R@1↑	R@5↑	R@10↑	MedR↓	R@1↑	R@5↑	R@10↑	MedR↓
MMT [17]	VT	7 experts	-	-	-	-	-	14.4	-	66
ActBERT [51]	VT	R101+Res3D	9.6	26.7	38.0	19	8.6	23.4	33.1	36
Support Set [40]	VT	R152+R(2+1)D-34	-	-	-	-	8.7	23.0	31.1	31
MIL-NCE [35]†	VT	I3D-G	11.4	30.6	42.0	16	9.4	22.0	30.0	35
MMV FAC [2]†	VAT	TSM-50x2	11.7	33.4	45.4	13	9.3	23.0	31.1	38
CLIP4Clip [5]	VT	CLIP	-	-	-	-	31.2	53.7	64.2	4
HT100M [36]	VT	R152+RX101	6.1	17.3	24.8	46	7.2	19.2	28.0	38
NoiseEstimation [5]	VT	R152+RX101	-	-	-	-	8.0	21.3	29.3	33
MIL-NCE* [35]	VT	R152+RX101	8.0	22.9	32.1	29	8.6	23.1	30.8	33
Ours	VT	R152+RX101	9.0	23.2	32.5	30	9.7	23.2	30.7	32
FC Baseline	VAT	R152+RX101	15.5	31.0	40.0	22	7.8	17.8	25.2	50
Self-Attention Baseline	VAT	R152+RX101	13.8	29.3	36.2	34	8.9	22.3	30.1	41
AVLNet [41]	VAT	R152+RX101	19.9	36.1	44.3	16	8.3	19.2	27.4	47
MCN [11]	VAT	R152+RX101	18.1	35.5	45.2	-	10.5	25.2	33.8	-
Ours	VAT	R152+RX101	19.3	37.8	47.3	13	9.6	22.6	32.0	32
MIL-NCE [35]†	VT	S3D-G	15.1	38.0	51.2	10	9.9	24.0	32.4	29.5
Ours	VT	S3D-G	14.7	36.2	47.9	12	8.3	19.0	27.5	42
Ours	VAT	S3D-G	23.0	43.3	53.8	8	8.7	19.3	28.3	40

ples are defined by the transcription timestamps provided with the dataset.

4.2. Text-To-Video Retrieval

Datasets and Metrics The problem of text-to-video retrieval involves searching a pool of videos for a single video that corresponds to a given ground-truth text query. We evaluate zero-shot text-to-video retrieval on the YouCook2 [50] and MSR-VTT [46] datasets, which are common benchmark datasets for zero-shot video retrieval. The YouCook2 dataset consists of cooking instructional video clips with human-annotated text descriptions, and we use the validation set of 3.5k clips following prior work [35, 36]. The MSR-VTT dataset contains 10K video clips with human-annotated captions on various topics, and we use the test set of 1K video clips from [36]. For the retrieval task, we compute the euclidean distance between the text and video representations through the pretrained network to find e.g. the top video candidates for a given text sample. For both datasets, we report the recall metrics: R@1, R@5, R@10, and Median Recall (MedR).

Comparison with the state-of-the-art We report the results on the text-to-video retrieval task for YouCook2 and MSR-VTT in Table 1 for two cases, zero-shot text-to-video retrieval (VT) and zero-shot text-to-video+audio retrieval (VAT). We find that our method achieves strong performance when compared with prior approaches in both cases and on both downstream datasets. Notably, the addition of the audio modality leads to a large performance boost on YouCook2. However, we observe that systems trained in a multimodal setup may be more sensitive to domain shifts as compared to single modality tasks like image classification. As we are dealing with multiple modalities, the misalignment of only a single modality from the training data may lead to reduced performance of the model. This can be seen

Table 2. Evaluation of zero-shot temporal action localization. MIL-NCE* uses the same training procedure as [35] with different backbone features, † indicates trainable backbone.

Method	Visual Backbone	CrossTask			MYT		
		Recall†	IOD†	IOU†	Recall†	IOD†	IOU†
Cross-task (superv.) [52]	R152+I3D	31.6	-	-	-	-	-
Cross-task (weakly superv.) [52]	R152+I3D	22.4	-	-	-	-	-
ActBERT [51]	R101+Res3D	37.1	-	-	-	-	-
ActBERT [51]	+ Faster R-CNN	41.4	-	-	-	-	-
MIL-NCE [35]†	I3D-G	36.4	-	-	-	-	-
Mining: GRU (superv.) [27]	TSN	-	-	-	-	14.5	7.8
Mining: MLP (weakly superv.) [27]	TSN	-	-	-	-	19.2	9.8
HT100M [36]	R152+RX101	33.6	26.6	17.5	15.0	17.2	11.4
MIL-NCE* [35]	R152+RX101	33.2	30.2	16.3	14.9	26.4	17.8
MCN [11]	R152+RX101	35.1	33.6	22.2	18.1	32.0	23.1
Ours	R152+RX101	35.2	32.6	21.4	18.0	31.6	22.9
MIL-NCE [35]†	S3D-G	40.5	-	-	-	-	-
UniVL [32]†	S3D-G	42.0	-	-	-	-	-
Ours	S3D-G	43.2	35.4	23.1	22.1	34.2	25.4

in the comparison of the performance of different modality combinations of MSR/VTT. Yet, in this case, better performance can be reached by simply dropping the misaligned domain. On the other hand, when all modalities more closely resemble the training data, as is the case with YouCook2, there is generally a performance improvement.

4.3. Temporal Action Localization

Datasets and Metrics Given a set of action classes, the goal of temporal action localization is to predict the actions present at each time-step of the video. In this task, we compute the distance between the video representation and each action’s text representation to obtain a class prediction for each time-step of the video. We evaluate on the CrossTask [52] and Mining YouTube [27] datasets. CrossTask contains 2.7k instructional videos; each video frame is manually annotated using action steps/ordering for each task collected from *wikiHow*. The recall is calculated using the same inference procedure of [52]. The Mining YouTube dataset contains videos from five simple cooking recipes - “eggroll”, “fried egg”, “pancake”, “omelet”, and “scrambled egg”. The test set contains 50 videos from each task (250 in total) that are densely annotated with 512 classes comprised of verb-object pairs (94 unique verbs and 171 objects). For evaluation, we report the recall metric as well as the intersection over detection (IoD) [9] and intersection over union (IoU) metrics as outlined in [27]. The IoD metric is defined as $\frac{G \cap D}{D}$ and the IoU metric is defined as $\frac{G \cap D}{G \cup D}$, where G is the ground-truth action and D is the prediction.

Comparison with the state-of-the-art We present the results for the temporal action localization task in Table 2. When compared to methods with the R152+RX101 backbone feature extractor [11, 35, 36], we show strong performance across both datasets and all metrics. On CrossTask, our proposed method achieves improved recall compared to both MIL-NCE [36] and UniVL [32] when using the S3D-G backbone. Furthermore, our method outperforms the fully supervised baseline in [52] and the state-of-the-art weakly supervised approach [27] on the reported metrics in

Table 3. Evaluation of different types of routing functions as well as without routing for $C = 64$ number of capsules and a dimensionality of $d_1 = d_2 = 16$ including runtime and memory usage.

Method	YouCook2		MSRVTT		Memory Usage (GB)	Run-time (sec/batch)
	R@1	R@10	R@1	R@10		
No Routing	15.3	41.9	7.6	30.1	9.12	0.687
Dynamic Routing [42]	17.0	44.3	8.2	31.1	20.50	1.534
EM Routing [23]	5.8	24.2	5.7	21.8	19.13	1.272
Set Transformer [29]	16.5	40.0	8.4	30.0	9.11	0.707
Self-Attention (ours)	18.6	44.0	8.7	31.6	9.11	0.722

Table 4. Evaluation on different number of capsules for a dimensionality of $d_1 = 32$ and $d_2 = 256$. It shows that on the given dataset we reach saturation around $C = 128$ capsules.

Method	YouCook2		MSRVTT		Memory Usage (GB)	Run-time (sec/batch)
	R@1	R@10	R@1	R@10		
$C = 32$	18.5	45.0	8.0	29.2	9.15	0.730
$C = 64$	18.1	46.1	8.6	29.4	11.24	0.768
$C = 128$	19.3	47.3	9.3	30.9	15.97	0.879
$C = 256$	18.7	46.5	8.7	30.5	27.98	1.096

CrossTask and Mining YouTube, respectively.

4.4. Ablations

Here, we present ablations to evaluate our proposed self-attention based routing mechanism’s efficacy, its ability to scale with more capsules, and compare with other architectural baselines. Additional ablations are contained in the appendix.

Routing We compare the proposed self-attention routing with previous routing methods including dynamic [42], EM [23], and Set Transformer [29] routing, as well as with a setup without any routing (i.e. learning a MLP to obtain existence probabilities). As dynamic and EM routing involve a computationally expensive iterative procedure and EM routing requires matrix capsules, we reduce the size of the network and fix the number of capsules to $C = 64$ and the dimensionality of the primary and secondary capsule to $d_1 = d_2 = 16$ to allow for a training with same batch size for all approaches. From the results shown in Table 3, we see that training with routing tends to outperform the respective baseline architectures without routing mechanisms. Among the evaluated methods, only the EM routing algorithm does not seem to be well suited for the targeted setup, as it suffers greatly from instability during training. In fact, all routing methods, including the proposed approach, tend to have some level of instability in this multimodal training paradigm, requiring the need for fine-tuning of learning rates. However, we find that our method, closely followed dynamic routing, suffer least from this instability and are able to achieve relatively strong performance in this experimental setup. One problem with iterative routing procedures, including dynamic routing, is that it becomes difficult to scale, mainly because of the larger memory footprint. Here, especially in the direct compar-

Table 5. Evaluation using fully connected and self-attention baselines.

Modalities	YouCook2				MSR-VTT			
	R@1	R@5	R@10	Med. R	R@1	R@5	R@10	Med. R
Fully Connected	15.5	31.0	40.0	22	7.8	17.8	25.2	50
Self-Attention	13.8	29.3	36.2	34	8.9	22.3	30.1	41
Ours	19.3	37.8	47.3	13	9.3	21.4	30.9	37

son with dynamic routing, the proposed method is able to achieve better results with fewer computational resources.

Number of Capsules To show the ability of the proposed routing mechanism to scale, we also analyse how the number of capsules effects our proposed architecture. For these experiments, we maintain the capsule dimension of the original training setting with $d_1 = 32$ and $d_2 = 256$ while varying the number of capsules, $C = 32, 64, 128, 256$. As shown in Table 4, increasing the number of capsules generally leads to an improvement in performance. This can be seen as a indicator that a larger number of capsules allows the network to capture more object or concept representations. With the current dataset, we find that our models saturate at $C \geq 128$; when the number of capsules becomes larger, we find that there is a diminishing return on performance. Considering computational efficiency, it further shows that even for large numbers of capsules, the run-time is still below that of the iterative routing mechanisms.

Comparison with Fully Connected and Self-Attention Baselines Since our main contribution is the proposal of a capsule-based framework for multimodal learning, we compare with other architecture baselines in Table 5. For a standard baseline, we have run an experiment which takes the input features and passes them through two fully connected layers (Fully Connected). It achieves lower performance than our proposed capsule network, showing that using capsules is valuable in learning multi-modal representations. We also compare with self-attention without capsule structures. For this experiment, we apply a multi-head self-attention layer on the input features. We take the input features and group the activations into N equal length vectors. Here, $N = 128$ so that it is as similar to the number of capsules in our main experiments. These vectors are used as the sequence for a self-attention layer, which is followed by a fully-connected layer to obtain the final feature representation for each modality. We find that self-attention outperforms the fully connected baseline on MSR-VTT, but does not reach the performance of our proposed self-attention routing method.

4.5. Qualitative Analysis

In our final set of evaluations, we attempt to understand what the proposed architecture is able to learn by analysing a set of qualitative retrieval examples as well as studying



Figure 3. Qualitative retrieval examples: top-3 zero-shot text-to-video retrieval results on the YouCook2 dataset for the proposed approach with self-attention based routing, our approach without the routing mechanism, and MIL-NCE* (* indicates that we used the same backbone as in our model). Correct video colored in green.



Figure 4. Top-4 videos with the highest activation for the particular capsule on the MSR-VTT dataset. Labels: #number of capsule: assumed learned “concept”.

how individual capsule activations effect the final feature representation. We include additional qualitative results in the appendix.

Retrieval Results We present retrieval results for three models - our self-attention based routing method, our approach without routing, and MIL-NCE - in Figure 3. Each column consists of the top-3 predictions for the given text query. Generally, routing achieves strong performance and retrieves visually varied videos; on the other hand, MIL-NCE tends to focus on specific objects or low-level visual cues leading to visually similar retrievals. In the first example, MIL-NCE retrieves videos of “melt butter”, but the butter is melted in a pan and not an “oven”. Notably, our approach successfully handles the extremely specific query “Put three rings of ketchup and two rings of mustard on the

bottom bun” as shown in the second row.

What Individual Capsules Learn To further understand the entities or objects that are modeled, we examine the capsules’ activations \hat{p}_i^m (Equation 2) and show samples that have a high activation for a specific capsule. Ideally, if two samples have a high activation for the same capsule, then the entity that it represents should be present within both inputs. In the MSR-VTT dataset we select the videos which lead to high activations for various capsules; we observe that different capsules model semantically distinct concepts as seen in Figure 4. The capsules learn to represent a wide range of entities: from general concepts like “games”, “cooking”, and “outdoor activities”, to specific objects like “vegetables” and “cars”. We find that this behaviour is consistent across various datasets.

5. Conclusion

In this work, we proposed a novel multimodal capsule network that learns to model various entities within given modalities and maps them to a joint embedding space. To learn from a large amount of noisy video data, we present a scalable self-attention based capsule routing mechanism, which we show outperforms previous routing methods on this task. Furthermore, we find that the capsules are able to learn representations of various concepts and objects within each modality. Our comprehensive experimental evaluation demonstrates the effectiveness of our approach on two downstream zero-shot tasks on four datasets.

References

- [1] Karim Ahmed and Lorenzo Torresani. Star-caps: Capsule networks with straight-through attentive routing. In *Advances in Neural Information Processing Systems*, 2019. 3
- [2] Jean-Baptiste Alayrac, Adria Recasens, Rosalia Schneider, Relja Arandjelović, Jason Ramapuram, Jeffrey De Fauw, Lucas Smaira, Sander Dieleman, and Andrew Zisserman. Self-supervised multimodal versatile networks. In *Advances in Neural Information Processing Systems*, 2020. 1, 2, 6
- [3] Humam Alwassel, Dhruv Mahajan, Bruno Korbar, Lorenzo Torresani, Bernard Ghanem, and Du Tran. Self-supervised learning by cross-modal audio-video clustering. *arXiv preprint arXiv:1911.12667*, 2019. 1
- [4] Humam Alwassel, Dhruv Mahajan, Bruno Korbar, Lorenzo Torresani, Bernard Ghanem, and Du Tran. Self-supervised learning by cross-modal audio-video clustering. In *Advances in Neural Information Processing Systems*, 2020. 2
- [5] Elad Amrani, Rami Ben-Ari, Daniel Rotman, and Alex Bronstein. Noise estimation using density estimation for self-supervised multimodal learning. *arXiv preprint arXiv:2003.03186*, 2020. 2, 6
- [6] Yuki Markus Asano, Christian Rupprecht, and Andrea Vedaldi. Self-labelling via simultaneous clustering and representation learning. *arXiv preprint arXiv:1911.05371*, 2019. 2
- [7] Mohammad Taha Bahadori. Spectral capsule networks. *ICLR Workshop*, 2018. 3
- [8] Angie W Boggust, Kartik Audhkhasi, Dhiraj Joshi, David Harwath, Samuel Thomas, Rogério Schmidt Feris, Danny Gutfreund, Yang Zhang, Antonio Torralba, Michael Picheny, et al. Grounding spoken words in unlabeled video. In *CVPR Workshops*, 2019. 2
- [9] Piotr Bojanowski, Rémi Lajugie, Francis Bach, Ivan Laptev, Jean Ponce, Cordelia Schmid, and Josef Sivic. Weakly supervised action labeling in videos under ordering constraints. In *ECCV*, 2014. 6
- [10] Joao Carreira and Andrew Zisserman. Quo vadis, action recognition? a new model and the kinetics dataset. In *CVPR*, 2017. 2, 5
- [11] Brian Chen, Andrew Rouditchenko, Kevin Duarte, Hilde Kuehne, Samuel Thomas, Angie Boggust, Rameswar Panda, Brian Kingsbury, Rogerio Feris, David Harwath, et al. Multimodal clustering networks for self-supervised learning from unlabeled videos. *ICCV*, 2021. 2, 6
- [12] Marco Cuturi. Sinkhorn distances: Lightspeed computation of optimal transport. *NeurIPS*, 26:2292–2300, 2013. 2
- [13] Jia Deng, Wei Dong, Richard Socher, Li-Jia Li, Kai Li, and Li Fei-Fei. Imagenet: A large-scale hierarchical image database. In *CVPR*, 2009. 2, 5
- [14] Jianfeng Dong, Xirong Li, Chaoxi Xu, Shouling Ji, Yuan He, Gang Yang, and Xun Wang. Dual encoding for zero-example video retrieval. In *Proceedings of the IEEE/CVF Conference on Computer Vision and Pattern Recognition*, 2019. 2
- [15] Kevin Duarte, Yogesh S Rawat, and Mubarak Shah. Video-capsulenet: A simplified network for action detection. *arXiv preprint arXiv:1805.08162*, 2018. 2
- [16] Marzieh Edraki, Nazanin Rahnnavard, and Mubarak Shah. Subspace capsule network. In *Proceedings of the AAAI Conference on Artificial Intelligence*, 2020. 3
- [17] Valentin Gabeur, Chen Sun, Karteek Alahari, and Cordelia Schmid. Multi-modal transformer for video retrieval. In *ECCV*, 2020. 2, 6
- [18] Taeyoung Hahn, Myeongjang Pyeon, and Gunhee Kim. Self-routing capsule networks. In *Advances in Neural Information Processing Systems*, 2019. 3
- [19] Kensho Hara, Hirokatsu Kataoka, and Yutaka Satoh. Can spatiotemporal 3d cnns retrace the history of 2d cnns and imagenet? In *CVPR*, 2018. 5
- [20] David Harwath, Adria Recasens, Dídac Surís, Galen Chuang, Antonio Torralba, and James Glass. Jointly discovering visual objects and spoken words from raw sensory input. In *ECCV*, 2018. 5
- [21] Kaiming He, Xiangyu Zhang, Shaoqing Ren, and Jian Sun. Deep residual learning for image recognition. In *CVPR*, 2016. 1, 5
- [22] Geoffrey E Hinton, Alex Krizhevsky, and Sida D Wang. Transforming auto-encoders. In *Proceedings of the International conference on artificial neural networks*, 2011. 2
- [23] Geoffrey E Hinton, Sara Sabour, and Nicholas Frosst. Matrix capsules with em routing. In *International conference on learning representations*, 2018. 2, 3, 7
- [24] Gabriel Ilharco, Yuan Zhang, and Jason Baldridge. Large-scale representation learning from visually grounded untranscribed speech. *arXiv preprint arXiv:1909.08782*, 2019. 4
- [25] Diederik P Kingma and Jimmy Ba. Adam: A method for stochastic optimization. *arXiv preprint arXiv:1412.6980*, 2014. 5
- [26] Adam R Kosiorek, Sara Sabour, Yee Whye Teh, Geoffrey E Hinton, and Miss Jo STAFFORD-TOLLEY. Stacked capsule autoencoders. *NeurIPS*, 2019. 2, 3
- [27] Hilde Kuehne, Ahsan Iqbal, Alexander Richard, and Jürgen Gall. Mining youtube-a dataset for learning fine-grained action concepts from webly supervised video data. *arXiv preprint arXiv:1906.01012*, 2019. 2, 6
- [28] Rodney LaLonde, Ziyue Xu, Ismail Irmakci, Sanjay Jain, and Ulas Bagci. Capsules for biomedical image segmentation. *Medical image analysis*, 2021. 2

- [29] Juho Lee, Yoonho Lee, Jungtaek Kim, Adam Kosior, Seungjin Choi, and Yee Whye Teh. Set transformer: A framework for attention-based permutation-invariant neural networks. In *Proceedings of the International Conference on Machine Learning*, 2019. 3, 7
- [30] Jie Lei, Linjie Li, Luowei Zhou, Zhe Gan, Tamara L Berg, Mohit Bansal, and Jingjing Liu. Less is more: Clipbert for video-and-language learning via sparse sampling. *arXiv preprint arXiv:2102.06183*, 2021. 2
- [31] Stuart Lloyd. Least squares quantization in pcm. *IEEE transactions on information theory*, 28(2):129–137, 1982. 2
- [32] Huaishao Luo, Lei Ji, Botian Shi, Haoyang Huang, Nan Duan, Tianrui Li, Xilin Chen, and Ming Zhou. Univlm: A unified video and language pre-training model for multimodal understanding and generation. *arXiv preprint arXiv:2002.06353*, 2020. 2, 6
- [33] Vittorio Mazzia, Francesco Salvetti, and Marcello Chierberg. Efficient-capsnet: Capsule network with self-attention routing. *arXiv preprint arXiv:2101.12491*, 2021. 3
- [34] Bruce McIntosh, Kevin Duarte, Yogesh S Rawat, and Mubarak Shah. Visual-textual capsule routing for text-based video segmentation. In *CVPR*, 2020. 2
- [35] Antoine Miech, Jean-Baptiste Alayrac, Lucas Smaira, Ivan Laptev, Josef Sivic, and Andrew Zisserman. End-to-end learning of visual representations from uncurated instructional videos. In *CVPR*, 2020. 1, 6
- [36] Antoine Miech, Dimitri Zhukov, Jean-Baptiste Alayrac, Makarand Tapaswi, Ivan Laptev, and Josef Sivic. Howto100m: Learning a text-video embedding by watching hundred million narrated video clips. In *ICCV*, 2019. 1, 2, 5, 6
- [37] Tomas Mikolov, Kai Chen, Greg Corrado, and Jeffrey Dean. Efficient estimation of word representations in vector space. *arXiv preprint arXiv:1301.3781*, 2013. 5
- [38] Ishan Misra and Laurens van der Maaten. Self-supervised learning of pretext-invariant representations. In *Proceedings of the IEEE/CVF Conference on Computer Vision and Pattern Recognition*, 2020. 5
- [39] Aaron van den Oord, Yazhe Li, and Oriol Vinyals. Representation learning with contrastive predictive coding. *arXiv preprint arXiv:1807.03748*, 2018. 4
- [40] Mandela Patrick, Po-Yao Huang, Yuki Asano, Florian Metz, Alexander Hauptmann, João Henriques, and Andrea Vedaldi. Support-set bottlenecks for video-text representation learning. *arXiv preprint arXiv:2010.02824*, 2020. 2, 6
- [41] Andrew Rouditchenko, Angie Boggust, David Harwath, Dhiraj Joshi, Samuel Thomas, Kartik Audhkhasi, Rogerio Feris, Brian Kingsbury, Michael Picheny, Antonio Torralba, et al. Avlnet: Learning audio-visual language representations from instructional videos. In *Interspeech*, 2021. 1, 2, 4, 6
- [42] Sara Sabour, Nicholas Frosst, and Geoffrey E Hinton. Dynamic routing between capsules. *arXiv preprint arXiv:1710.09829*, 2017. 1, 2, 3, 7
- [43] Ramon Sanabria, Ozan Caglayan, Shruti Palaskar, Desmond Elliott, Loïc Barrault, Lucia Specia, and Florian Metz. How2: a large-scale dataset for multimodal language understanding. *arXiv preprint arXiv:1811.00347*, 2018. 2
- [44] Chen Sun, Austin Myers, Carl Vondrick, Kevin Murphy, and Cordelia Schmid. Videobert: A joint model for video and language representation learning. In *Proceedings of the IEEE/CVF International Conference on Computer Vision*, 2019. 2
- [45] Aisha Urooj Khan, Hilde Kuehne, Kevin Duarte, Chuang Gan, Niels Lobo, and Mubarak Shah. Found a reason for me? weakly-supervised grounded visual question answering using capsules. *arXiv e-prints*, 2021. 2
- [46] Jun Xu, Tao Mei, Ting Yao, and Yong Rui. Msr-vtt: A large video description dataset for bridging video and language. In *Proceedings of the IEEE conference on computer vision and pattern recognition*, 2016. 2, 6
- [47] Min Yang, Wei Zhao, Jianbo Ye, Zeyang Lei, Zhou Zhao, and Soufei Zhang. Investigating capsule networks with dynamic routing for text classification. In *Proceedings of the 2018 conference on empirical methods in natural language processing*, 2018. 2
- [48] Suofei Zhang, Quan Zhou, and Xiaofu Wu. Fast dynamic routing based on weighted kernel density estimation. In *Proceedings of the International Symposium on Artificial Intelligence and Robotics*, 2018. 3
- [49] Yongheng Zhao, Tolga Birdal, Haowen Deng, and Federico Tombari. 3d point capsule networks. In *Proceedings of the IEEE/CVF Conference on Computer Vision and Pattern Recognition*, 2019. 2
- [50] Luowei Zhou, Chenliang Xu, and Jason Corso. Towards automatic learning of procedures from web instructional videos. In *Proceedings of the AAAI Conference on Artificial Intelligence*, 2018. 2, 6
- [51] Linchao Zhu and Yi Yang. Actbert: Learning global-local video-text representations. In *Proceedings of the IEEE/CVF Conference on Computer Vision and Pattern Recognition*, 2020. 2, 6
- [52] Dimitri Zhukov, Jean-Baptiste Alayrac, Ramazan Gokberk Cinbis, David Fouhey, Ivan Laptev, and Josef Sivic. Cross-task weakly supervised learning from instructional videos. In *Proceedings of the IEEE/CVF Conference on Computer Vision and Pattern Recognition*, 2019. 2, 6

A. Additional Ablations

Shared weights For our proposed architecture, we share weights across the various modalities after the initial capsules are extracted. Not only does this reduce the number of learned parameters for the network, but we find that it leads to learning improved representations. We present results in Table 6. Generally, for data more closely related to the training data (for example, evaluating on YouCook2) the use of shared weights leads to improved performance.

B. Self-attention Architectural Details

For our self-attention routing procedure we first use linear projections to generate the query-key-value. Given that

Table 6. Evaluation using shared weights

Modalities	YouCook2				MSR-VTT			
	R@1	R@5	R@10	Med. R	R@1	R@5	R@10	Med. R
Not Shared	16.8	35.4	44.6	15	9.5	22.8	30.3	30.5
Shared	19.3	37.8	47.3	13	9.6	22.6	32.0	32

there are C input capsules and the output capsules have dimension d_2 , the query, key, and value matrices have shape $Q, K, V \in \mathbb{R}^{C \times d_2}$. The output of the multi-head self-attention operation,

$$V' = \text{softmax} \left(\frac{QK^T}{\sqrt{d_2}} \right) V, \quad (6)$$

is a matrix of the same dimension. We then apply normalization across the columns (i.e. capsule feature dimension) as well as two fully connected linear layers, and dropout, with hidden dimension 1024 and output dimension d_2 . A residual connection from V' to the output capsule features, followed by normalization across the capsule feature dimensions.

C. Additional Qualitative Results

Retrieval Quality In the case of retrieval, we show three text queries together with their three closest video representations in Figure 5. It becomes clear that all video representations show a close match for the described scene. Additionally, one has to remark that the retrieved video examples for each query do show sufficient variance with respect to color, view point, and other low-level cues. This can be seen as an indicator that the learned clustering is based on some high-level common concepts rather than on the pure co-occurrence of low-level feature representations.

Retrieval Results We present additional retrieval results for three models - our self-attention based routing method, our approach without routing, and MIL-NCE - in Figure 6. Each column consists of the top-3 predictions for the given text query. Generally, routing achieves strong performance and retrieves visually varied videos; on the other hand, MIL-NCE tends to focus on specific objects or low-level visual cues leading to visually similar retrievals. The first three rows consist of examples where our self-attention based routing correctly retrieves videos but the other two methods do not. For general queries, like “grill the ribs” and “flip the pancakes” in the bottom two rows, there are many relevant videos to choose from. Only the no-routing method obtains the “correct” video in its top-3 predictions, but these “failure cases” for our method and MIL-NCE would be considered correct retrievals by human standards.

Capsule Activations In Figure 7, we include videos which correspond to various capsules’ highest activations

across three different datasets: HowTo100M, MSR-VTT, and YouCook2. The concepts tend to remain consistent across the different datasets. In the final three rows, we present examples where the concept does not exist within the target dataset: “repair”, “games”, and “pets/animals” are not present within the cooking dataset, YouCook2. Since these capsules learn to represent these specific concepts/entities, their highest activation corresponds to seemingly random videos.

“add oil vinegar lemon juice and garlic to a bowl”



“chop and add fresh basil and stir”



“mix flour baking powder and salt”



“marinate the ribs well with the prepared sauce in a bucket overnight”



Figure 5. Qualitative evaluation: examples of top-3 zero-shot text-to-video retrieval results on the YouCook2 dataset. Correct video colored in green.

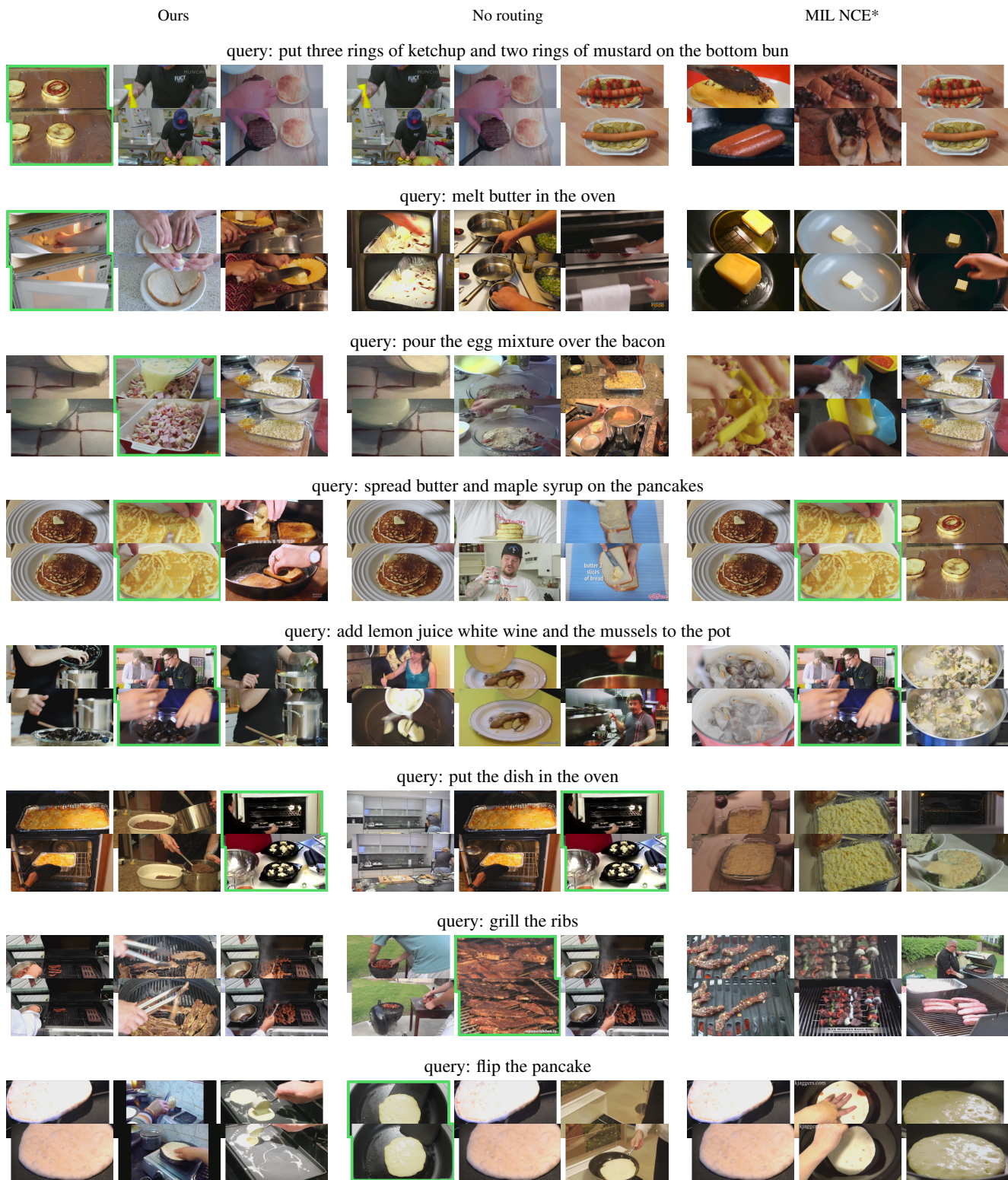


Figure 6. More qualitative examples: top-3 zero-shot text-to-video retrieval results on the YouCook2 dataset for the proposed approach with self-attention based routing, the same one but without routing mechanism, and MIL-NCE* (* indicates that we used the same backbone as in our model). Correct video colored in green.

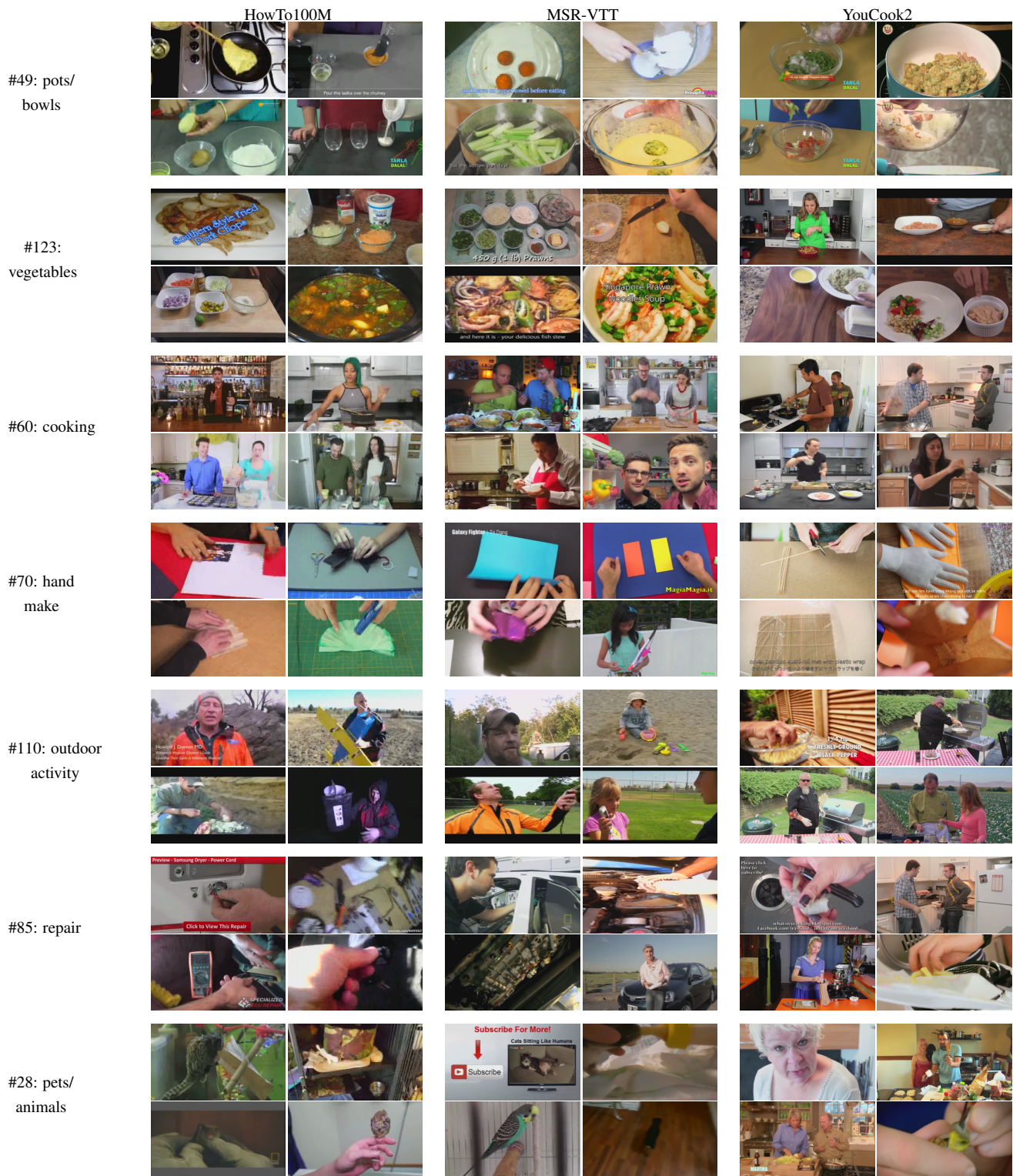


Figure 7. Extended figure with examples of capsule highest activations: top-4 videos with the highest activation for the particular capsule for the HowTo100M, MSR-VTT, and YouCook2 datasets. Labels: #number of capsule: assumed learned “concept”.